

# Ferrite Content and Morphology of type 308 Stainless Steel Weld Metal

H.I. Shaaban,\* M.A. Shafey and F.H. Hammad  
Atomic Energy Establishment  
Cairo, Egypt

## ABSTRACT :

The variations of both ferrite number (FN) and morphology of Type AISI 308 deposited weld metal were studied. The predicted means of population of FN values at the top, transverse and longitudinal sections were estimated as 7, 5 and 5, respectively. The variation in FN values was attributed to various reasons such as the orientation of ferrite phase from section to section, weld metal solidification rate, cooling rate, and the dissolution of the ferrite phase due to subsequent thermal cycles in a multipass weld metal.

The morphology of the ferrite phase was investigated metallographically and found to vary from bead to bead. Three different morphologies were distinguished, namely vermicular, lacy and globular.

## 1. Introduction :

The effect of ferrite in reducing hot cracking susceptibility of austenitic stainless steel weld metal is well established (Refs. 1-3). It was found that 3-8 per cent is required to reduce hot cracking (Refs. 4, 5). This relationship between ferrite content and weld cracking has led to the development of codes which require ferrite in welds to be above specific minimum level. For example, the American Society of Mechanical Engineers boiler and pressure vessel code (Ref. 6) requires 5% minimum of ferrite content in austenitic stainless steel weldments.

Using the alloying content of the welding electrodes, many empirical diagrams, such as Schaeffler (Ref. 7) and DeLong (Ref. 8), and empirical formulas, such as Seferian formula (Ref. 9), were developed to determine ferrite content in the filler metal. Such diagrams and formulas were found helpful in predicting the amount of delta ferrite in stainless steel weld metal.

\* At present on leave to the Office of Inspection and Enforcement, U.S. Nuclear Regulatory Commission, Washington, D.C.

However, recent studies (Refs. 10-12) showed that the ferrite content is not a sufficient condition to prevent cracking. The morphology and distribution of the ferrite phase is also necessary to produce an optimal weld strength. Ferrite may be found in various morphologies and distributions depending on the welding parameters. Thus, it may be inaccurate to predict ferrite content from strictly alloying composition, without taking into consideration the morphology and distribution of the ferrite phase.

In the present study Magne Gauge measurements were used to determine the ferrite content at the three orthogonal faces of deposited weld metal. The variation in ferrite content from one face to another was detected. Also, metallography was used for studying the various morphologies of the weld metal microstructure.

## 2. Experiment :

Commercial rutile-coated shielded metal arc welding electrodes were used to deposit the weld metal beads. The chemical composition of the 8 swg diameter electrodes are given in Table 1. The manual shielded metal arc (SMA) welding process was used. The welding conditions were the downhand position, 130 A (DC), electrode positive (RP). The multipass deposited weld metal beads (120 x 120 x 20 mm) was deposited on a fixed plate of Type AISI 304 stainless steel. Fig.1 shows the assembly prepared to prevent the warpage of the deposited weld metal. The deposit was air cooled and then cut into cubic specimens 16 mm on a side.

Table 1

The chemical composition of the stainless steel electrodes Type AISI 308

C	Si	Mn	Cr	Ni	Fe
0.06	0.29	0.58	19.75	9.9	balance

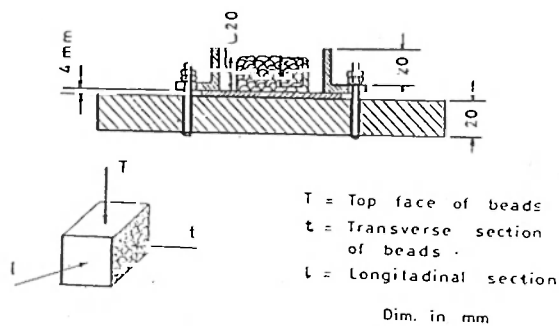


Fig. 1: Preparation of deposited weld metal specimens

FN values of the weld metal were determined using a Magne Gauge instrument which was calibrated by National Bureau of Standards according to the American Welding Society standard AWS-A4-74. Ten readings were made on each of the three polished faces of all the specimens. The cubic specimens were prepared for metallographic examination by using an electrolytic polished technique described by Bell and Sonon (Ref. 13).

### 3. Results and Discussion :

#### 3.1 Ferrite Content Measurements :

The mean values and standard deviations of FN of the three orthogonal faces for 12 cubic specimens prepared from one multipass bead of Type AISI 308 stainless steel deposited weld metal are shown in Table 2. The values given are the average of 10 Magne Gauge readings taken on each individual face of any of the cubes. Table 2 also shows the arithmetic mean and the mean of population of the FN value of the weld metal with confidence level of 98% over the three orthogonal faces of the bead.

The results show that the values of FN vary from point to point in the same orthogonal face of any of the cubic specimens. However, the standard deviation for all the 10 readings was found to be less than 1 FN in most of the cases. Also the values of FN vary from one specimen to another and it is usually higher at the top surface (the top bead of the weld metal) compared to the other two faces (the longitudinal and transverse directions). The top face has, on the average, an increase of about 2 FN which represents 40% of the longitudinal and transverse values.

Table 2

Average values, standard deviation and predicted mean of FN for 12 specimens on the three orthogonal faces

Specimen No.	The orthogonal face		
	top	transverse	longitudinal
1.	7.7±1.0	5.4±0.9	5.3±1.2
2.	6.3±0.7	4.7±0.9	4.3±1.2
3.	8.5±0.6	4.2±1.6	3.5±2.1
4.	6.7±0.4	5.9±0.8	5.2±0.9
5.	5.7±1.2	2.8±0.9	5.3±0.8
6.	6.3±0.8	5.4±0.7	4.5±0.8
7.	5.9±0.7	3.4±0.6	3.5±0.4
8.	4.9±0.8	3.0±0.5	4.2±1.0
9.	6.5±1.1	-----	3.9±0.5
10.	5.4±0.7	4.7±0.8	4.9±0.7
11.	6.4±0.7	4.6±1.4	4.2±0.6
12.	4.6±0.8	4.1±0.5	2.8±2.0
X	6.24	4.38	4.30
U	7	5	5

Where X = The arithmetic average of FN of all specimens at each orthogonal section.

U = The mean of population with confidence level 98%.

The variation of the mean values of FN in the same orthogonal face for the various samples or from point to point at the same face of one sample could be attributed to various reasons. One of these reasons is the change in composition within the same bead due to segregation of alloying elements during freezing. Since the ferrite phase is a non-equilibrium phase (Fig.2), thus it may be highly cored (Ref. 14), i.e., microsegregation will take place. This microsegregation depends on whether the first solid formed is austenite or ferrite. Lippold and Savage (Ref. 15) showed that alloys with compositions on the low Cr-side of the liquidus (top of three phase triangle of Fig.3) solidify as primary austenite dendrites. Alloys with compositions on the high Cr-side of the liquidus solidify as primary delta-ferrite dendrites. This will result in a variation on FN readings at various points of the same orthogonal face.

Another reason of this variation in FN values could be due to the variation of cooling rate

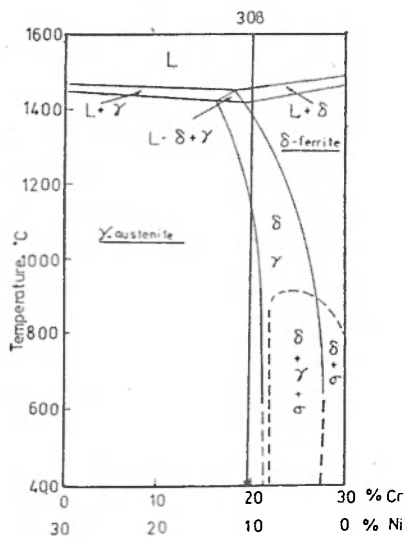
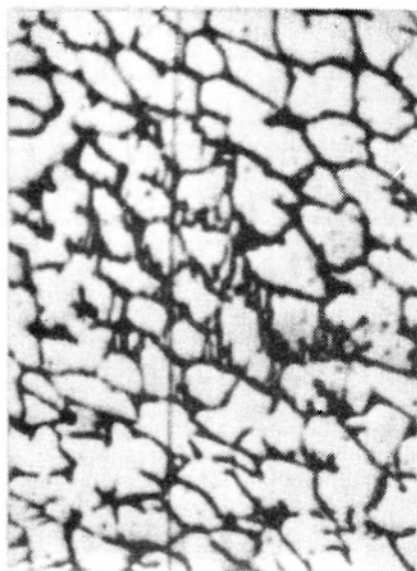


Fig. 2: 70% vertical section of the Fe-Cr-Ni ternary phase diagram showing the approximate composition of Type 308 stainless steel



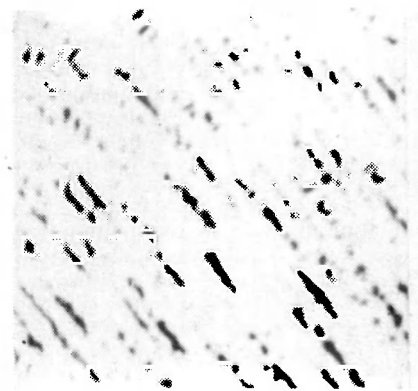
(a) Vermicular

from point to point. Lipold and Savage (Ref. 16) showed that higher cooling rate increases the ferrite content and affects the morphology of the ferrite phase.

Small nitrogen variations strongly affect delta ferrite content in austenitic stainless steel weld metal. The nitrogen is known to be an austenitizer with Ni equivalent varies



(b) Lacy



(c) Globular

Fig.3: Various Ferrite Morphologies Observed in Deposited Weld Metal

between 8-45 (Ref. 17). The amount of nitrogen pickup varies from one welding process to another (0.02% in GRAW and 0.04% in GMAW) (Ref. 18). However, much higher pick up is possible if the gas shielding protection is poor.

The increase in the FN value at the top face of the weld metal specimens could be attributed to the orientation of the ferrite with respect to the surface. The effect of orientation size, and shape of ferrite upon measuring the FN by Magne Gauge have been reported. Simpkinson (Ref. 19) used a specific percentage of iron powder press-formed into powdered metal compacts and found that the coarse iron powder gave higher FN readings than the fine powder of the same percentage. In the present study, if it is assumed that the actual ferrite content in the three surfaces is the same, it would be expected that the ferrite is coarser in the top face.

The observed difference in FN value between top face and the other two faces could also

be attributed to the effect of annealing of subsequent weld passes. The ferrite may be dissolved in the lower passes as a result of annealing (Ref. 20) by the subsequent thermal cycles. This decreases the ferrite content at the root passes compared to the top passes. Such explanation was confirmed by David (Ref. 21) who attributed the drastic reduction of FN in the root passes to the dissolution of ferrite by the subsequent weld passes.

### 3.2 Ferrite Morphology :

No typical microstructure of the ferrite in the multipass austenitic weld metal could be detected. Fig. 3 shows various microstructures of weld metal at different passes. Three types of ferrite morphologies could be distinguished which are known as vermicular, lacy, and globular shape.

The vermicular shape is the one in which the ferrite appears as an aligned skeletal Network or as curved soft form (Fig. 3a). This shape exists frequently in the austenitic weld metal containing duplex structure (Refs. 21-23). The ferrite in the vermicular shape could be located within the cores of the primary and secondary dendrite arms and is the result of either the incomplete primary transformations or location at the cell boundaries. If the weld metal solidifies as a primary delta-ferrite dendrites, the cores are highly enriched in chromium and depleted in nickel. Upon cooling through the two-phase region (austenite + ferrite), the ferrite formed during steady state solidification transforms to austenite either by composition invariant as a massive transformation (Ref. 24) or by a controlled diffusion process. However, a portion of the ferrite at the dendrite cores is sufficiently enriched in Cr and depleted in Ni to remain stable at room temperature and is characterized by the vermicular morphology as suggested by Lippold and Savage (Ref. 16). If the weld metal solidifies as primary austenitic, and the delta ferrite solidifies from the rest, then the melt between cells will be an eutectic ferrite (Ref. 25) and delta-ferrite appears as a vermicular morphology (Ref. 23).

Vitek and David (Ref. 26) investigated solidification behaviour of Type 308 stainless steel welds. They showed that the primary solidification phase was the ferrite phase and the only morphology was vermicular for submerged arc and shielded metal arc welds.

The lacy morphology, shown in Fig. 3b, is characterized by a lace shape, i.e., line patterned net-like structure twisted over and under each other. The ferrite network is oriented along

the growth direction in an austenite matrix. It looks very regular and aligned. David (Ref. 21) observed the lacy ferrite morphology in the multipass weld metal and proposed that the origin of this ferrite morphology is the transformation of primary delta-ferrite cells to widmanstätten austenite and ferrite. David and co-workers (Ref. 27) had investigated the solidification behaviour of Type 308 stainless steel filler metal using the interrupted solidification technique. In this technique, the weld metal was slowly cooled from 1,365°C to below the solidus temperature and the water quenched. The lacy shape was detected in the weld metal prepared in such manner. The mechanism they proposed for the appearance of the lacy morphology is that the volume fraction of primary delta-ferrite continues to increase as the temperature decreases below liquidus. At 1,387°C austenite begins to envelop the primary delta-ferrite. This enveloped primary delta-ferrite is transformed to widmanstätten structure, which leads to the appearance of the so-called lacy morphology.

Fredricksson (Ref. 28) observed lacy shape in 18/8 stainless steel ingots and attributed it to the transformation of primary solidified ferrite to widmanstätten austenite. Lippold and Savage (Refs. 15, 16) suggested that a massive transformation of ferrite to austenite is impossible in high ferrite welds. Consequently a diffusion-controlled transformation must occur upon cooling through the two-phase region. Thus the as-welded microstructure consisted of the lacy ferrite and widmanstätten austenite.

Type 308 weld metal is known to have low ferrite content ( $C_{req}/N_{req} = 1.76$ ). However, ferrite phase of lacy morphology was detected. This could be attributed to the local fluctuations in both the alloy composition and the weld cooling rate along the solidification front. This may lead to a change in the transformation mechanism and results in mixed microstructure as suggested by Lippold and Savage (Ref. 16).

The third ferrite morphology detected in the present study was the globular morphology (Fig. 3c). The globular shape is characterized by ferrite in the form of spheres distributed in a matrix of austenite. This morphology is not related to the solidification mode. It appears mostly at the weld passes which are subjected to the thermal cycles. These thermal cycles lead to the transformation of a part of the ferrite to austenite (Ref. 21). Such transformation process is followed by changing of delta-ferrite morphology from the as-solidified morphology (vermicular or lacy) to the globular one.

David (Ref. 21) was able to detect the

appearance of the globular morphology by the annealing at high temperature of ferrite having other thermally instable morphologies. Also heat treatment at temperatures between 600-900°C of deposited Type 308 stainless steel weld metal yielded the appearance of this globular ferrite morphology (Ref. 20).

Another ferrite morphology which was detected by other investigators (Refs. 21, 26) in Type 308 weld metal is the acicular morphology. The acicular morphology is a needle-like ferrite distributed in an austenite matrix. However, such morphology was not detected in the present study. Viteck and David (Ref. 26) proved that the acicular morphology appears in Type 308 weld metal only if the GTA welding process is used. This may be due to the difference in the cooling rates between the SMA welding process used in the present study and the GTA process. If we propose that the cooling rate in SMA process is lower, this will lead to the transformation of the needle-shaped acicular ferrite to small disconnected spheres (globular ferrite morphology).

#### 4. Conclusions

1. Different values of FN were observed by measuring the magnetic flux in the three orthogonal sections of 308 type weld metal. The difference was attributed to variation in orientation of ferrite phase, solidification and cooling rates and dissolution of ferrite phase during the subsequent welding thermal cycles.

2. Ferrite content at the top face was found to be 7 FN which is 2 FN higher than the value for other two orthogonal faces (5 FN).

3. Vermicular and lacy morphologies of ferrite appeared in the ferrite phase of Type 308 weld metal due to the solidification mode and the transformation followed by solidification. The globular morphology of ferrite phase is due to dissolution of any of the previous shapes as a result of the subsequent thermal cycles.

#### Acknowledgement :

One of the authors (H.I.S.) appreciates the International Atomic Energy Agency fellowship offered to him during which most of this paper was written.

#### References :

1. Barland, J.C., and Younger, R.N. (1960). Some Aspects of Cracking in Welded Cr-Ni Austenitic Steels. *British Welding J.*, F(1) : 22-60
2. Hull, F.C., 1967. Effect of Delta Ferrite in Hot Cracking of Stainless Steel. *Welding J.*, 46(9) : 399S-409S
3. Lundin, C.D., and Spond, D.F., 1976. The Nature and Morphology of Fissures in Austenitic Stainless Steel Weld Metals. *Welding J.*, 55(11) : 356S-367S.
4. Brooks, J.A., and Lambert, Jr., F.J., 1978. The Effect of Phosphorus, Sulfur and Ferrite Content on Weld Cracking of Type 309 Stainless Steel. *Welding J.*, 57(5) : 139S-143S.
5. DeLong, W.T., 1975. Ferrite in Austenitic Stainless Steel Weld Metal. *Indian Welding J.*, May : 33-42.
6. AWS-A5.4 Specifications for Covered Corrosion-Resisting Chromium and Chromium-Nickel Steel Welding Electrodes (1981).
7. Schaeffler, A.L., 1948. Welding Dissimilar Metals with Stainless Electrodes. *Iron Age*, July 1. 162 : 72
8. DeLong, W.T., and Reid, Jr., H.F., 1957. Properties of Austenitic Chromium and Austenitic Chromium-Manganese Stainless Steel Weld Metal. *Welding J.*, 37(1) : 1-8
9. Seferian, D., 1959. *Metallurgie de la Soudure*, Denod, Paris
10. Suutala, N., 1983. Effect of Solidification Condition Mode in Austenitic Stainless Steel. *Met. Trans.*, 14A : 191-197.
11. Sundar, L., 1984. The Relation Between Solidification Mode Ferrite Morphology and Fissuring in Austenitic Stainless Steel Weldments. *Indian Welding J.*, January : 32-41.
12. Kujanpaa, V.P., 1984. Weld Discontinuities in Austenitic Stainless Steel Sheet - Effect of Impurities and Solidification Mode. *Welding J.*, 63(12) : 369S-375S.
13. Bell, C., and Sonon D.E., 1976. 9 : 91-96
14. Kujanpaa, V.P., Suutala, N.J., Takalo, T.K. and Moisia, T.J., 1980. Solidification Cracking Estimation of the Susceptibility of Austenitic and Austenitic Ferritic Stainless Steel Welds. *Metal Construction*, 12(6) : 282-285.
15. Lippold, J.C., and Savage, W.F., 1979. Solidification on Austenitic Stainless Steel Weldments - Part 1, a Proposed Model. *Welding J.*, 58(12) 362S-374S

16. Lippold, J.C. and Savage, W.F., 1980. Solidification of Austenitic Stainless Steel Weldments - Part 2, The Effect of Alloy Composition on Ferrite Morphology. *Welding J.*, 59(2) : 48S-58S
17. Norozhilov, N.M., et al., 1978. On the Austenitizing and Ferritizing Effect of Elements in Austenitic Ferrite Weld Metals. *Welding Production*, (6) : 12-13.
18. Long, C.J., and DeLong, W.T., 1973. The Ferrite Content of Austenitic Stainless Steel Weld Metal. *Welding J.*, 52(7) : 281S-297S.
19. Simpkinson, T., 1952, *Iron Age*, 166
20. Shafey, M.A., Shaaban, H.I., El-Sabagh, A.S., and Hammad, F.H., 1984. Post Weld Heat Treatment of Austenitic Stainless Steel Weldments. First Ein-Shams Univ. Conference PEDD, Cairo, Dec. 24-27. Conference proceedings page 421.
21. David, S.A., 1981. Ferrite Morphology and Variation in Ferrite Content in Austenitic Stainless Steel Welds. *Welding J.*, 60(4) : 63S-71S.
22. Goodwin, G.M., Cole, N.C., and Slaughter, G.M., 1972. A Study of Ferrite Morphology in Austenitic Stainless Steel Weldments. *Welding J.*, 51(9), 425S-429S.
23. Suutala, N., Takalo, T., and Moisio, T., 1979. The Relationship Between Solidification and Microstructure in Austenitic and Austenitic-Ferritic Stainless Steel Welds. *Met. Trans.* 10A : 512-514.
24. Suutala, N., Takalo, T., and Moisio, T., 1981. Technical Note : Comment on the Transformation  $\delta$ - $\gamma$  by a Massive Mechanism in Austenitic Stainless Steel. *Welding J.*, 61 : 92S-93S.
25. Cieslak, M.J., Ritter, A.M., and Savage, W.F., 1982. Solidification Cracking and Analytical Electron Microscopy of Austenitic Stainless Steel Weld Metals. *Welding J.*, 61(1) : 1S-8S.
26. Vitek, J.M., and David, S.A., 1984. The Solidification and Aging Behaviour of Types 308 and 308 CRE Stainless Steel Welds. 63(8) : 247-253.
27. David, S.A., Goodwin, G.M., and Braski, D.N., 1979. Solidification Behaviour of Austenitic Stainless Steel Filler Wire. *Welding J.*, 59(11) : 330S-336S.
28. Fredriksson, H., 1972. *Met. Trans.*, A3 : 2989